GRAPHENE SYNTHESIS VIA ELECTROCHEMICAL EXFOLIATION OF GRAPHITE NANOPLATELETS IN AQUEOUS SULFURIC ACID

Lin Li-Shang[1], Aidan Westwood[1], Rik Brydson[1]

[1]School of Chemical and Process Engineering, University of Leeds, LS2 9JT, UK

INTRODUCTION

Graphene, a two-dimensional honeycomb sp^2 carbon lattice has received enormous attention because of the potential for various applications such as the electrodes of photovoltaic devices and batteries, next generation flexible electronics and even antibacterial coatings [1][2]. Interest in the application of graphene is mainly due to its high electrical conductivity, flexibility and huge tuneability of the properties of graphene-based materials [3][4]. For example, the semi-metal character of pristine graphene can be changed to semiconducting [5], insulating [6] or superconducting [7] by control of size or chemical functionalization.

To utilize graphene's unique properties and potential adaptability, several graphene synthesis methods have been developed. Mechanical exfoliation is the earliest technique to isolate monolayer graphene, but the yields are limited. Chemical Vapour Deposition (CVD) epitaxial growth exploits catalytic metal substrates such as Ni or Cu and can produce large area and high-quality graphene directly on the substrate, but the requirements of high temperature and the multi-step transferral process are major difficulties for cheap, industrial-scale production [4][8]. Chemical exfoliation of graphene using Hummers' method is attractive for producing solution-processed graphene oxide (GO), but subsequent chemical or thermal treatments can only partially remove its oxygen content so that electrical properties cannot be fully restored [9][8]. Numerous other synthesis techniques have been developed to overcome these limitations, including solvent-assisted Liquid-Phase Exfoliation (LPE) [10][8] or the formation of graphite intercalation compounds [11], but extensive sonication processes are required that limit the size and yield of thin graphene flakes [4]. Furthermore, due to its low solubility, the exfoliated graphene is usually dispersed in high-boiling-point solvents, which creates difficulties for subsequent film preparation. Therefore a low-cost, solution-processable method that can lead to high-quality graphene film is desirable [4].

In this work, we intend to compare the properties of graphene flakes manufactured from Liquid Phase Exfoliation (LPE) and electrochemical exfoliation (ECE) of graphite. The electrochemical exfoliation of graphite is performed in dilute sulphuric acid, the resulting electrochemically exfoliated graphene flakes (EG) were characterized by Raman spectroscopy, Dynamic Light Scattering (DLS), Transmission Electron Microscopy (TEM) and Selective Area Electron Diffraction (SAED), and compared with the raw material and also with Liquid Phase Exfoliated (LPE) graphene. The results reveal that high-quality graphene flakes can be obtained from this and simple, fast and cost-effective electrochemical exfoliation approach.

METHODOLOGY

Graphene synthesis using an electrochemical cell

To understand the relative effectiveness of electrochemical exfoliation, exfoliated graphene materials were manufactured using two different routes for comparison: (1) Liquid Phase Exfoliation (LPE) and (2) Electrochemical Exfoliation (ECE). For liquid phase exfoliation, the graphite raw material (graphite nanoplatelets (GNP), provided by Cheaptubes^{TM}) was exfoliated and dispersed in in Isopropyl alcohol (IPA) after 13 days of sonication (Bransonic 1510, 40 kHz, 80W). In contrast, the electrochemical exfoliation utilised pressed-GNP starting material as an electrode and were manufactured by pressing graphite nanoplatelets (GNP) in a 2.54 cm diameter with 0.4 ton of pressing force for 300 seconds. A two-electrode electrochemical cell was set up for the electrochemical exfoliation, with a platinum (Pt) cathode and pressed-GNP graphite anode and 0.1M sulphuric acid was used as the electrolyte. A constant potential of 10V was applied to initiate the exfoliation. The exfoliation process took around 3 min. and the exfoliated graphene flakes were washed with DI water and collected via centrifugation and then dispersed in IPA.

Material Characterization

X-ray Diffraction (XRD) and Scanning Electron Microscopy (SEM) were initially used to investigate the morphology and crystallography of the raw material (i.e. GNP) as well as the pressed-GNP electrode, The exfoliated graphene flakes were characterized by Dynamic Light Scattering (DLS) to obtain the lateral size distribution and Transmission Electron Microscopy (TEM) was used to study their morphology. Raman spectroscopy and TEM/Selected Area Electron Diffraction (SAED) were employed to investigate the crystalline structure and identify the number of layers in the graphene flakes. Raman spectroscopy was performed with a 532 nm excitation laser on LPE and ECE graphene flakes deposited on a Si substrate. TEM samples were prepared by drop casting the IPA dispersions onto holey amorphous carbon-coated copper TEM grids and allowing them to dry.

RESULTS AND DISCUSSION

As shown in Fig. 1(a), a two-electrode electrochemical cell was set up for the electrochemical exfoliation. The 10 V DC potential is believed to drift electrolyte anions into grain boundaries or defect sites within the pressed graphite electrode and subsequently these intercalate into the graphene platelets. This static potential is continuously applied for 180 seconds, which triggers the electrochemical reaction ($\mathbf{SO_4^{2-}_{(aq)}+4H^+ + 2e^- \rightarrow SO_{2\,(g)} + 2H_2O}$). Consequently, this gas evolution causes graphene flakes to peel off from the graphite electrode. A clear change of the electrolyte is observed from colourless to dark after only a few minutes of exfoliation (fig. 1a). SEM images from the raw GNP material and the pressed-GNP electrode are shown in fig.1 (b). The GNP powder is seen to consist of many small graphite flakes stacking on top of each other, with a lateral flake size of few micrometres. In contrast the pressed-GNP electrode has a smooth surface morphology, however the surface texture and flake boundaries are still apparent. X-Ray diffraction of the GNP powder and the pressed-GNP electrode are presented in Fig.1(c). The (002) diffraction peak of the pressed-GNP electrode is much more intense than that of the raw GNP material, indicating that pressing had induced a preferred orientation of the graphite nanoplatelets.

DLS, TEM, and SAED were employed to compare the morphology and crystalline structure of the graphene samples. The lateral size distribution of the LPE and ECE graphene samples was studied by DLS (Figures 2 (a) and 2(b)). The DLS plot suggests that the lateral size of the LPE samples ranged from ca. 0.4 μm to 2 μm, whilst the ECE samples demonstrated a narrower size distribution, from ca. 0.6 μm to 1.2 μm, implying that the flake size distribution is more controllable using electrochemical exfoliation. TEM images are shown in Figures 2 (c) and 2(d) and thin graphene flakes can be found in both samples. However, no monolayer graphene flake was found within the 21 selected flakes from LPE sample, the (inset) SAED patterns show that the LPE graphene is polycrystalline, meaning many grain boundaries, sub-flakes or defects are contained within the graphene flakes (Fig. 2 (c)). As shown in (Fig. 2 (d)), the ECE graphene, in contrast, 1 monolayer graphene flake were found out of 19 selected flakes under TEM, which exhibits a typical 6-fold symmetric diffraction pattern with stronger diffraction from the (0-110) planes than from the

(1-210) planes, indicative of a highly crystalline single layer graphene at the area in the TEM image selected for measurement (denoted by the red circles) [11][12].

Raman spectroscopy was also used to characterize the crystalline structure and quality of the graphene samples. In addition, the number of graphene layers can be estimated by the shape of the Raman 2D peak. Figure 3 presents the Raman spectra of the pressed-GNP electrode, LPE graphene, and ECE graphene. The two main features evident in the spectra are: the G band at ~1590 cm^{-1} , related to first-order scattering of the E_{2g} vibrational mode of sp^2 carbon, the relative intensity of which reflects the degree of graphitization [13]; and the D band at ~1350 cm^{-1} arising from the breathing mode of the sp^2 atom-based rings and enhanced by the existence of defects, grain boundaries, functional groups or structural disorder [14][8]. The Raman spectrum of the pressed graphite shows a prominent G peak (Intensity ratio of the D to G peak, I_D/I_G=0.24), whereas the LPE graphene reveals a high D band intensity (I_D/I_G=0.89), that could be caused by defects generated by the sonication process. The Raman spectrum of ECE graphene shows much lower D band intensity, with I_D/I_G=0.46, which suggests a much lower level of defects or disorder than in the LPE graphene. In addition, the shape of the 2D band at ~2680cm^{-1} is known to change with the number of graphene layers [1][14] and a peak analysis procedure was used to quantify the bandshape change to estimating the number of graphene layers (Figure 4 inset [13], [15]–[17]). The 2D peak was de-convoluted into four vibrational elements, $2D_{1B}$, $2D_{1A}$, $2D_{2A}$, $2D_{2B}$, two of which, $2D_{1A}$ and $2D_{2A}$, have higher relative intensities than the other two, as indicated in fig.4 inset. The ratio of integrated area: $(2D_{2A}+2D_{2B})$ / $(2D_{1B} + 2D_{1A})$ (indicated as A_{D2}/A_{D1} in fig.4) was plot versus the number of graphene layers. Well established data was taken from Ferrari's previous work [14] for regression reference, using this method, the ECE graphene was estimated to comprise of between 3-5 layers from three of the randomly selected flakes, whereas the LPE graphene flakes comprise more than 5 layers using the same sampling method. It is noteworthy that estimating the number of graphene layers could be inaccurate, because factors such as vibrational signals from the flake edge, stacking order or tilted baseline from scattering could affect the 2D peak bandshape, which could cause inaccuracy of the estimated number of layers.

The proposed mechanism of electrochemical exfoliation is shown in Figure 5. The SO_4^{2-} anions diffuse to the interface between electrolyte and graphite electrode under the influence of the applied electrical potential, become inserted into the graphite via grain boundaries and subsequentially intercalate between the graphite layers. Electrochemical reactions occur in this intercalation space and cause the formation of SO_2 bubbles that expand and cause the thin graphene layers to peel off (Fig. 5(a)). From the SEM image of the graphite electrode following electrochemical exfoliation (Fig.5 (b)), it is clear that surface roughness had increased (compared with the pristine electrode surface in figure 1(b)).

CONCLUSION

In conclusion, we have employed a simple, fast and cost–effective approach to prepare high quality graphene flakes via the electrochemical exfoliation of a pressed GNP graphite electrode. The electrochemically exfoliated graphene flakes showed fewer defects and higher crystallinity than graphene flakes prepared by Liquid Phase Exfoliation.

Figure 1 illustrates the electrochemical exfoliation of pressed graphite. (a) Experimental setup (left) and exfoliation of pressed graphite (right). (b) SEM secondary electron images of graphite nanoplatelets (GNP) (left), and the surface morphology of the pressed-GNP electrode (right). (c) XRD of the starting GNP material and the pressed-GNP electrode.

Figure 2 shows the DLS data revealing the lateral platelet size distribution of: (a) LPE graphene and (b) electrochemical exfoliated graphene. TEM images and (inset) SAED patterns of (c) LPE and (d) electrochemically exfoliated graphene.

Figure 3 Raman spectra of pressed graphite, LPE graphene, and electrochemically exfoliated graphene. The inset shows the ratio of peaks $2D_1$ and $2D_2$ which changes with the number of layers.

Figure 4 Shows the ratio of Raman peaks $2D_1$ and $2D_2$ which changes with the number of layers, estimated number of layers from ECE and LPE were labelled in the graph. Inset shows 2D peak was de-convoluted into four vibrational elements, $2D_{1B}$, $2D_{1A}$, $2D_{2A}$, $2D_{2B}$, two of which, $2D_{1A}$ and $2D_{2A}$, have higher relative intensities than the other two.

Figure 5 (a) Proposed mechanism for electrochemical exfoliation of graphene; (b) SEM secondary electron image of graphite electrode surface following electrochemical exfoliation process.

ACKNOWLEDGMENT

This study is supported by the School of Chemical and Process Engineering, University of Leeds, Especially thank to Prof. Rik Brydson and Dr. Aidan Westwood, Dr. Aslam Zabeada, and Robert Simpson, Diane Cochane and Mo Javed

REFERENCES

[1] K. S. Novoselov, V. I. Fal'ko, L. Colombo, P. R. Gellert, M. G. Schwab, and K. Kim, "A roadmap for graphene.," *Nature*, vol. 490, no. 7419, pp. 192–200, Oct. 2012.

[2] J. Wu, H. a. Becerril, Z. Bao, Z. Liu, Y. Chen, and P. Peumans, "Organic solar cells with solution-processed graphene transparent electrodes," *Appl. Phys. Lett.*, vol. 92, no. 26, pp. 4–6, 2008.

[3] M. Hofmann, W.-Y. Chiang, T. D. Nguyễn, and Y.-P. Hsieh, "Controlling the properties of graphene produced by electrochemical exfoliation.," *Nanotechnology*, vol. 26, no. 33, p. 335607, Aug. 2015.

[4] K. Parvez, R. Li, S. R. Puniredd, Y. Hernandez, F. Hinkel, S. Wang, X. Feng, and K. Müllen, "Electrochemically exfoliated graphene as solution-processable, highly conductive electrodes for organic electronics," *ACS Nano*, vol. 7, no. 4, pp. 3598–3606, 2013.

[5] A. Nourbakhsh, M. Cantoro, T. Vosch, G. Pourtois, F. Clemente, M. H. van der Veen, J. Hofkens, M. M. Heyns, S. De Gendt, and B. F. Sels, "Bandgap opening in oxygen plasma-treated graphene.," *Nanotechnology*, vol. 21, no. 43, p. 435203, Oct. 2010.

[6] K.-J. Jeon, Z. Lee, E. Pollak, L. Moreschini, A. Bostwick, C.-M. Park, R. Mendelsberg, V. Radmilovic, R. Kostecki, T. J. Richardson, and E. Rotenberg, "Fluorographene: a wide bandgap semiconductor with ultraviolet luminescence.," *ACS Nano*, vol. 5, no. 2, pp. 1042–6, Feb. 2011.

[7] B. Uchoa and A. H. Castro Neto, "Superconducting states of pure and doped graphene.," *Phys. Rev. Lett.*, vol. 98, no. 14, p. 146801, Apr. 2007.

[8] K. Parvez, Z. S. Wu, R. Li, X. Liu, R. Graf, X. Feng, and K. Müllen, "Exfoliation of graphite into graphene in aqueous solutions of inorganic salts," *J. Am. Chem. Soc.*, vol. 136, no. 16, pp. 6083–6091, 2014.

[9] G. Eda, G. Fanchini, and M. Chhowalla, "Large-area ultrathin films of reduced graphene oxide as a transparent and flexible electronic material.," *Nat. Nanotechnol.*, vol. 3, no. 5, pp. 270–4, May 2008.

[10] Y. Hernandez, V. Nicolosi, M. Lotya, F. M. Blighe, Z. Sun, S. De, I. T. McGovern, B. Holland, M. Byrne, Y. K. Gun'Ko, J. J. Boland, P. Niraj, G. Duesberg, S. Krishnamurthy, R. Goodhue, J. Hutchison, V. Scardaci, A. C. Ferrari, and J. N. Coleman, "High-yield production of graphene by liquid-phase exfoliation of graphite.," *Nat. Nanotechnol.*, vol. 3, no. 9, pp. 563–568, Sep. 2008.

[11] L. Wei, F. Wu, D. Shi, C. Hu, X. Li, W. Yuan, J. Wang, J. Zhao, H. Geng, H. Wei, Y. Wang, N. Hu, and Y. Zhang, "Spontaneous intercalation of long-chain alkyl ammonium into edge-selectively oxidized graphite to efficiently produce high-quality graphene.," *Sci. Rep.*, vol. 3, p. 2636, Jan. 2013.

[12] Z. Sun, Z. Yan, J. Yao, E. Beitler, Y. Zhu, and J. M. Tour, “Growth of graphene from solid carbon sources.,” *Nature*, vol. 468, no. 7323, pp. 549–52, Nov. 2010.
[13] A. C. Ferrari, “Raman spectroscopy of graphene and graphite: Disorder, electron-phonon coupling, doping and nonadiabatic effects,” *Solid State Commun.*, vol. 143, no. 1–2, pp. 47–57, 2007.
[14] A. C. Ferrari, J. C. Meyer, V. Scardaci, C. Casiraghi, M. Lazzeri, F. Mauri, S. Piscanec, D. Jiang, K. S. Novoselov, S. Roth, and A. K. Geim, “Raman Spectrum of Graphene and Graphene Layers,” *Phys. Rev. Lett.*, vol. 97, no. 18, p. 187401, Oct. 2006.
[15] I. Childres, L. Jauregui, and W. Park, “Raman spectroscopy of graphene and related materials,” *... Phot. Mater. ...*.
[16] S. Reich and C. Thomsen, “Raman spectroscopy of graphite.,” *Philos. Trans. A. Math. Phys. Eng. Sci.*, vol. 362, no. 1824, pp. 2271–88, Nov. 2004.
[17] E. H. Martins Ferreira, M. V. O. Moutinho, F. Stavale, M. M. Lucchese, R. B. Capaz, C. a. Achete, and a. Jorio, “Evolution of the Raman spectra from single-, few-, and many-layer graphene with increasing disorder,” *Phys. Rev. B*, vol. 82, no. 12, p. 125429, Sep. 2010.

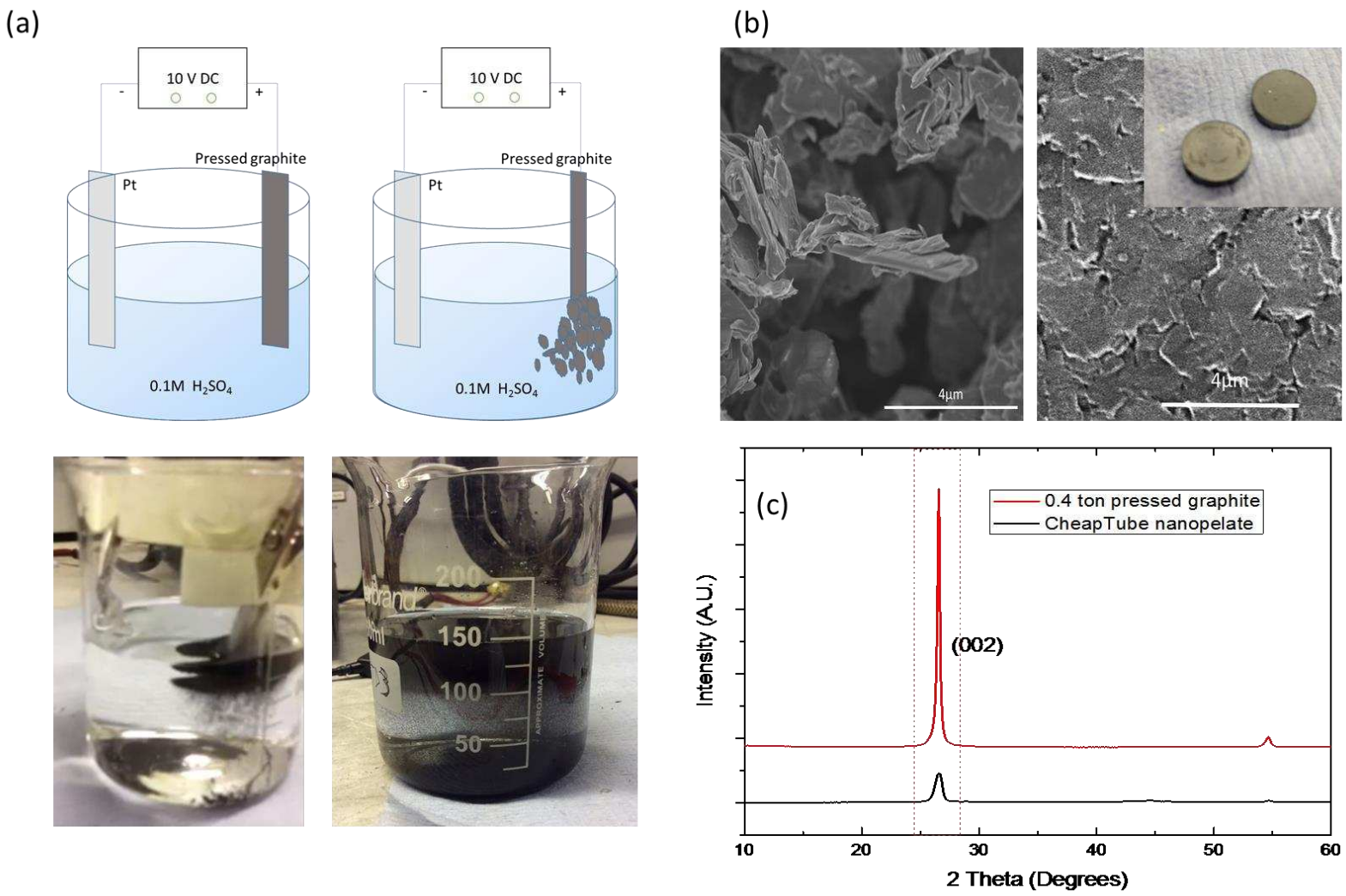

Figure 1 illustrates the electrochemical exfoliation of pressed graphite. (a) Experimental setup (left) and exfoliation of pressed graphite (right). (b) SEM secondary electron images of graphite nanoplatelets (GNP) (left), and the surface morphology of the pressed-GNP electrode (right). (c) XRD of the starting GNP material and the pressed-GNP electrode.

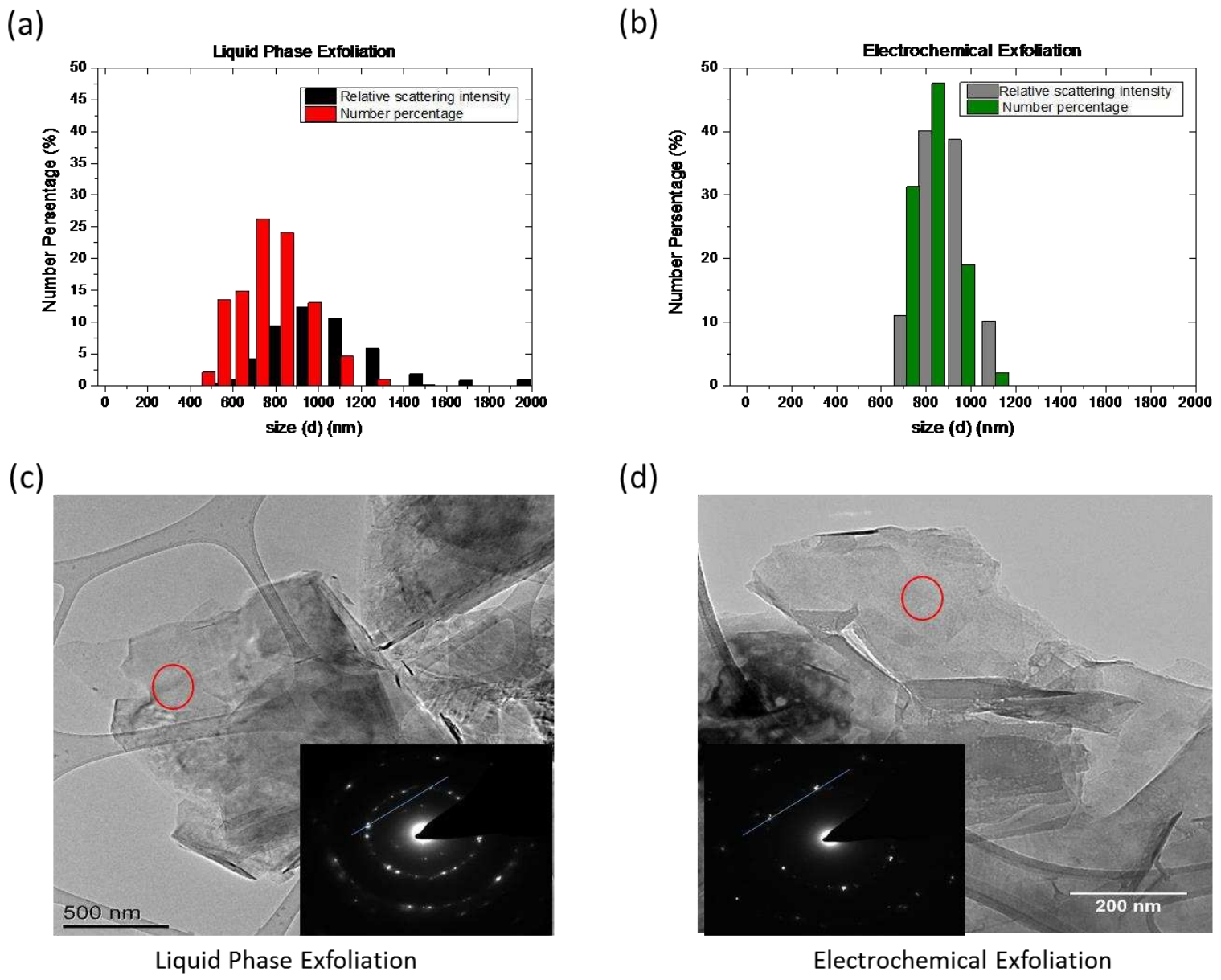

Figure 2: (Top) DLS. Lateral size distribution of (a) LPE graphene and (b) electrochemically exfoliated graphene. (Bottom) TEM image and SAED diffraction pattern of (c) LPE and (d) electrochemically exfoliated graphene

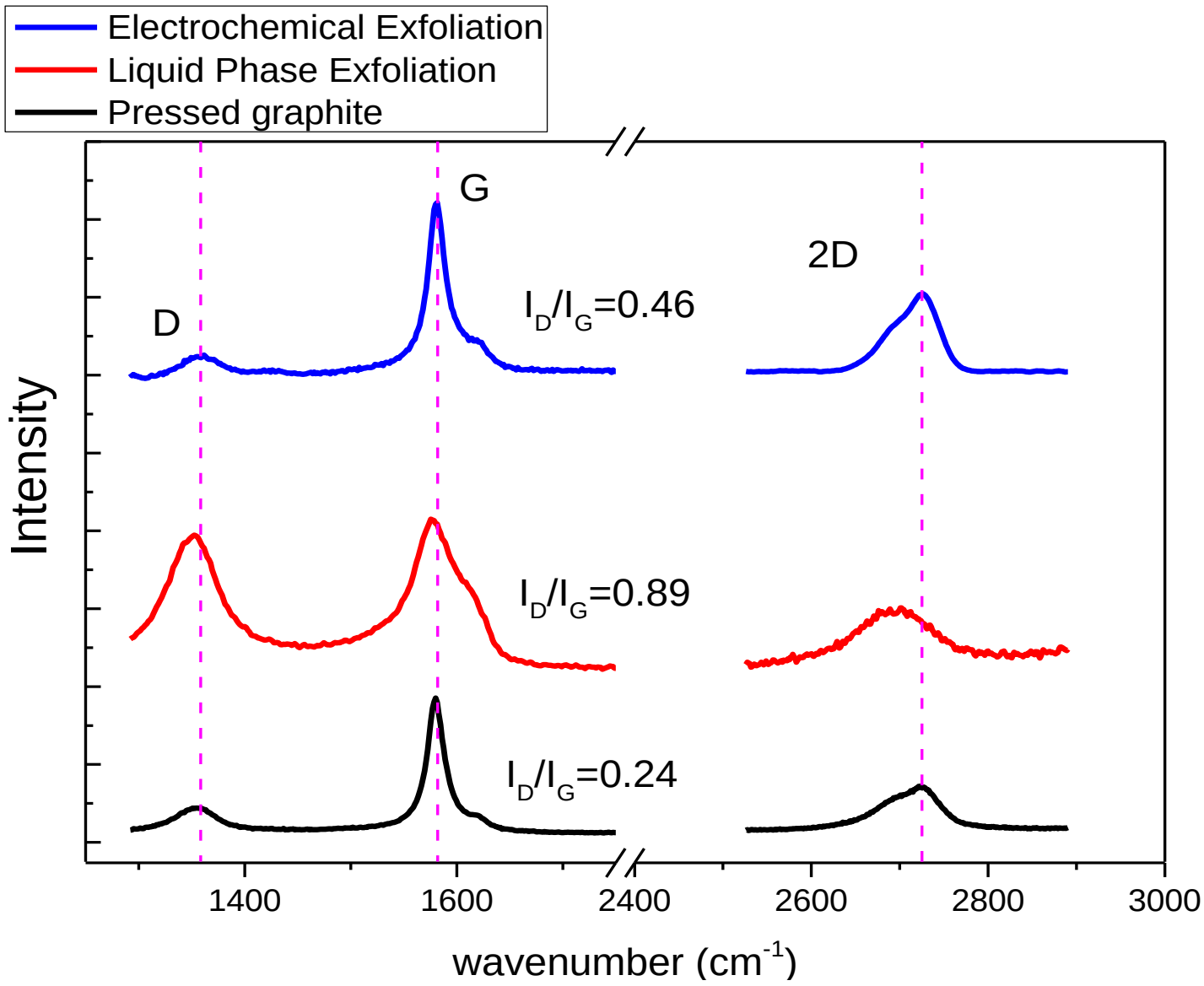

Figure 3 Raman spectra of pressed graphite, LPE graphene, and electrochemically exfoliated graphene.

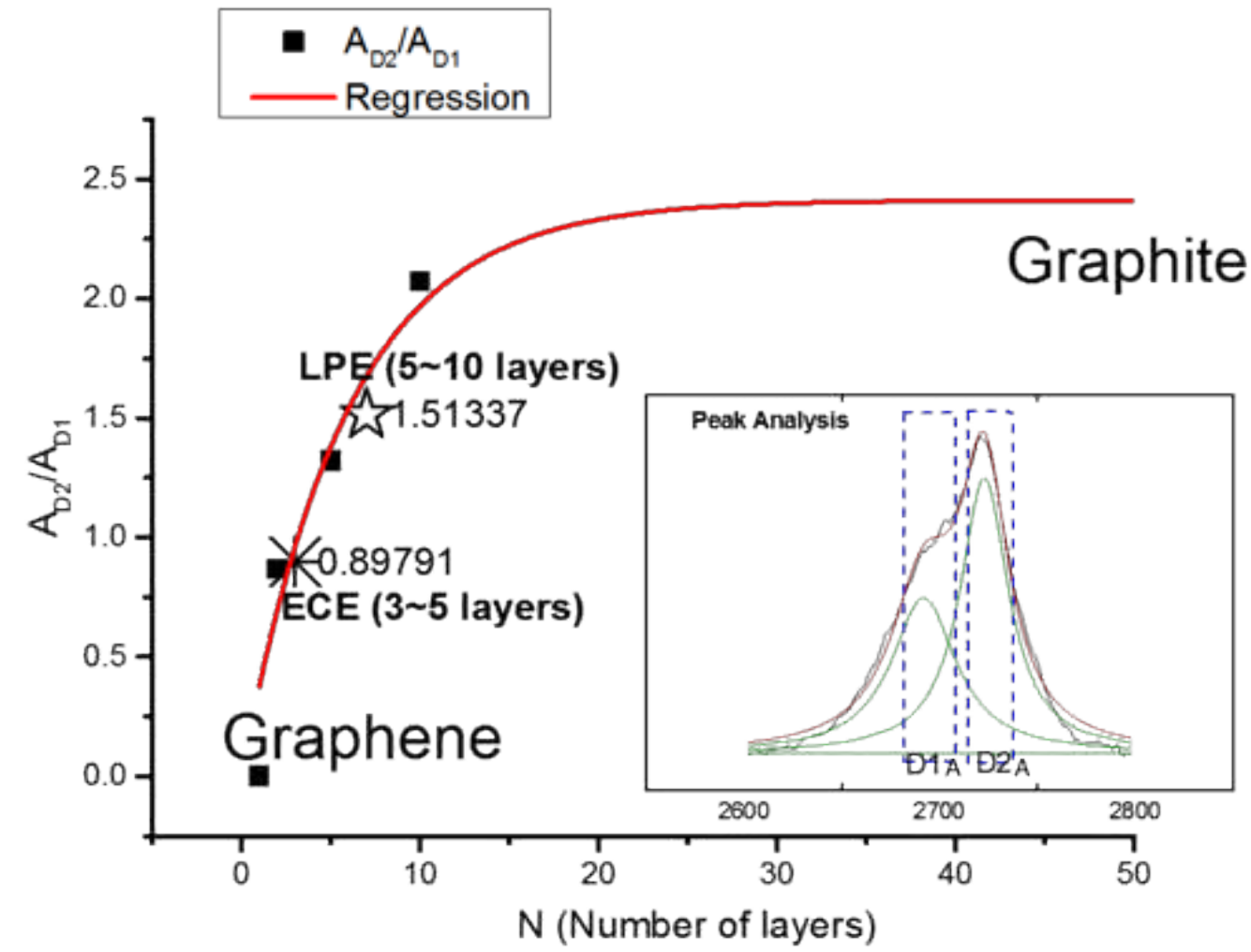

Figure 4 Shows the ratio of Raman peaks $2D_1$ and $2D_2$ which changes with the number of layers, estimated number of layers from ECE and LPE were labelled in the graph. Inset shows 2D peak was de-convoluted into four vibrational elements, $2D_{1B}$, $2D_{1A}$, $2D_{2A}$, $2D_{2B}$, two of which, $2D_{1A}$ and $2D_{2A}$, have higher relative intensities than the other two.

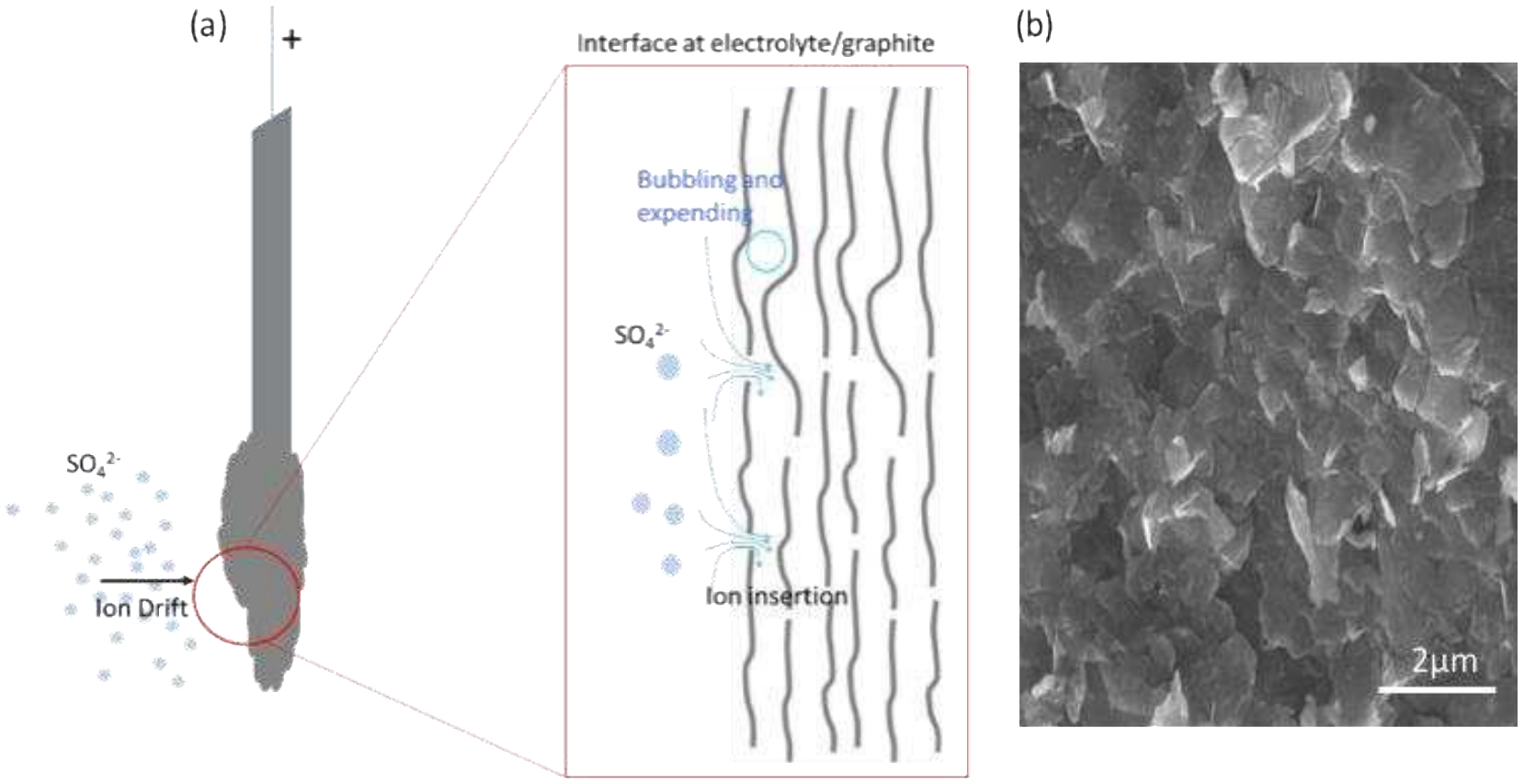

Figure 5: (a) proposed mechanism of electrochemical exfoliation. (b) SEM image of graphite electrode after electrochemical exfoliation process.